Eur Radiol (2017) 27:2391–2399
DOI 10.1007/s00330-016-4586-x

MAGNETIC RESONANCE

Whole-body MRI in patients with Non-bacterial Osteitis: Radiological findings and correlation with clinical data

A. P. Arnoldi[1] · C. L. Schlett[2] · H. Douis[3] · L. L. Geyer[1] · A. M. Voit[4] · F. Bleisteiner[4] · A. F. Jansson[4] · S. Weckbach[2]

Received: 23 October 2015 / Revised: 29 May 2016 / Accepted: 29 August 2016 / Published online: 23 September 2016

Abstract

Objectives To correlate clinical findings of Non-bacterial Osteitis (NBO) with whole-body MRI (WB-MRI) findings and determine a radiologic index for NBO (RINBO) which allows standardized reporting of WB-MRI.

Methods and materials In a prospective study, 40 patients with diagnosis of NBO underwent clinical examination and WB-MRI in which STIR- and T1- weighted images were assessed for NBO-typical lesions. Parameters of interest for RINBO were: number of radiologically active lesions (RAL), size of the patients' maximum RAL presence of extramedullary and spinal involvement. Results were tested for statistical agreement of clinical and MR-based lesion detection. RINBO was tested for correlation with clinical activity.

Results 62/95 clinically/radiologically active lesions were found in 30/33 patients. In 45 % of the cohort, more active lesions were detected by WB-MRI than by clinical examination. RINBO was a significant predictor for the presence of clinically active lesions.

Conclusion WB-MRI is a powerful diagnostic tool for patients with NBO which can reveal asymptomatic disease activity. With RINBO a standardized evaluation approach is proposed which helps assessing radiologic disease burden and predicts clinical disease activity.

Key Points

- *Whole body MRI is a powerful diagnostic tool for patients with non-bacterial Osteitis.*
- *Whole body MRI can reveal asymptomatic disease activity.*
- *The radiologic index RINBO offers a standardized evaluation approach.*

Keywords Whole body imaging · Magnetic resonance imaging · Non-bacterial Osteitis · CRMO · Activity score

Abbreviations

NBO	Non-bacterial Osteitis
CRMO	Chronic Recurrent Multifocal Osteomyelitis
WB-MRI	Whole Body Magnetic Resonance Imaging
RINBO	Radiologic index for Non-bacterial Osteitis
LMU	Ludwig-Maximilians-University
CAL	Clinically active lesions
VAS	Visual analogue scale
CRP	C-reactive protein
ESR	Erythrocyte sedimentation rate
STIR	Short tau inversion recovery
DWI	Diffusion weighted Imaging
RAL	Radiologically active lesions
RNAL	Radiologically not active lesions
SI	Signal intensity
POI	Parameter of interest
lpp	Lesions per patient
AUC	Area under the curve

A. F. Jansson and S. Weckbach contributed equally to this work.

✉ A. P. Arnoldi
Andreas.Arnoldi@med.uni-muenchen.de

[1] Institute for Clinical Radiology, Ludwig-Maximilians-University Hospital, Nussbaumstrasse 20, 80336 Munich, Germany

[2] Diagnostic and Interventional Radiology, University Hospital Heidelberg, Heidelberg, Germany

[3] Department of Radiology, University Hospital Birmingham, Birmingham B15 2TH, United Kingdom

[4] Department of Rheumatology & Immunology, Dr. von Hauner Children's Hospital, Ludwig-Maximilians-University, Munich, Germany

Introduction

Non-bacterial Osteitis (NBO) is a rare (0.4 per 100.000 [1]) but most likely under-diagnosed disease usually affecting children and adolescents [2, 3] mostly taking a chronic course formerly known as chronic recurrent multifocal osteomyelitis (CRMO). While an auto-inflammatory process with a genetic susceptibility is assumed, the exact aetiology and pathogenesis still remain unclear [4, 5]. Patients usually present with non-specific clinical symptoms of focal or multifocal bone pain sometimes associated with local swelling or overheating. Also serum biomarkers and histopathologic findings lack sensitivity and specificity limiting their diagnostic value [1, 6–9]. Therefore, the diagnosis of NBO usually remains a diagnosis of exclusion after ruling out other diseases such as infective osteomyelitis, Langerhans-cell histiocytosis, Ewing's-sarcoma, osteosarcoma or leukaemia. Radiography can show bone lesions with osteolysis and sclerotic margins, but frequently fails to demonstrate a discernible lesion. Given the osteomyelitic pathophysiology, targeted MRI can add valuable information about solitary lesions [10], nevertheless, lesions of uncertain aetiology frequently require bone biopsy. Whole-body MRI (WB-MRI) recently offers a more comprehensive imaging approach allowing assessment of multiple disease affected areas in one setting and in a non-invasive manner. WB-MRI has already proven its value for the evaluation of multifocal malignant, endocrine or rheumatologic diseases [11–16] and the latest studies highlight the potential of WB-MRI to detect typical patterns of bone involvement and subclinical lesions in NBO but emphasize the variable appearance of the disease [17–19]. This led us to the idea of implementing a scoring system in order to ease the reporting, improve the reproducibility and simplify the validation and staging of the disease. While only few studies with small cohorts attempted to directly correlate MRI with clinical findings [18–20], the clinical impact of imaging findings on patient management is an ongoing debate.

Therefore, the aim of this study is to correlate clinical with WB-MRI findings of NBO patients and to determine a radiologic index for NBO (RINBO) which allows standardized reporting.

Methods

Ethics

The study was approved by the ethics committee of the medical faculty of the Ludwig-Maximilians-University (LMU) Munich, Germany. All patients gave written informed consent.

Study cohort

In this prospective study, patients were recruited from a tertiary paediatric care centre between January 2010 and April 2011. Inclusion criteria were NBO diagnosed according to published criteria [1, 21] and willingness to participate. A subgroup ($n = 17$) of this collective with a disease history of more than 10 years has been the subject of a previously published study on clinical long-term assessment of disease activity [22]. Exclusion criteria were MRI non-compatible metal implants and claustrophobia. Patients were examined clinically at the Dr. von Hauner Childrens Hospital, LMU, and subsequently underwent WB-MRI at the Institute of Clinical Radiology, LMU within a mean time period of 8 (±21 SD; range: 0-66) days.

Clinical examination

Patients were interviewed and examined by a rheumatologist (A.J.; more than 5 years of experience in paediatric rheumatology). Anatomical areas, which demonstrated symptoms of pain, swelling or heating within the last two weeks were defined as clinically active lesions (CAL). The number of lesions, their anatomic locations and the associated intensity of local pain on the visual analogue scale (VAS) (range: 0-10; with 0 no pain and 10 maximum pain) were documented. Laboratory tests were performed in a subset of our patients measuring C-reactive protein (CRP) (≥0.5 mg/dl pathologic) in 26 patients (65 %) and erythrocyte sedimentation rate (ESR) (≥15 mm/h pathologic) in 24 patients (60 %).

WB-MRI imaging protocol

WB-MRI was performed at a 3 Tesla Scanner (Magnetom Verio, Siemens Medical Solutions, Erlangen, Germany) equipped with 32 receiver channels. Patients were positioned head first supine and covered with a head and neck coil, spine array coils and three body coils (total imaging matrix, TIM, Siemens Medical Solutions). Upper arms were positioned parallel to the chest, lower arms and hands were positioned upon the pelvis covered by an additional body coil. A disease-adapted scanning protocol (Table 1) acquired overlapping coronal ($n = 5$-6) and sagittal ($n = 2$) short tau inversion recovery (STIR) and non-contrast T1-weighted (w) turbo spin-echo sequences in subsequent table positions. Additional axial diffusion weighted imaging (DWI) sequences with b values of 800 were obtained in 11 patients, but the results were not included in the current analyses.

Image analysis

MR exams were assessed in consensus reading by two radiologists (S.W., H.D.; both with more than 5 years of

Table 1 Sequence parameters of Whole-Body MRI protocol

	T1-w TSE coronal	STIR SPC coronal	T1-w TSE sagittal	STIR SPC sagittal
TR (ms)	783	4000	700	6000
TI (ms)	-	210	-	210
TE (ms)	12	326	11	48
Matrix [phase x read]	384 × 307	320 × 259	448 × 358	384 × 326
Resolution [phase x read x slice] (mm^3)	1.1 × 1.1 × 5.0	1.5 × 1.5 × 5.0	1.1 × 0.9 × 3.5	1.2 × 1.0 × 3.5
FOV (mm^2)	480 × 336	480 × 336	400 × 400	400 × 400
Flip angle (°)	180	T2 var	180	180
Bandwidth (Hz/px)	161	1116	180	250
Parallel imaging method	GRAPPA	GRAPPA	GRAPPA	GRAPPA
Respiratory compensation	Free breathing	Free breathing	Free breathing	Free breathing
Acquisition time (s)	106 × 6	88 × 6	81 × 2	155 × 2

experience in musculoskeletal MRI) using a standard PACS-workstation (Syngo Imaging; Siemens Medical Solutions) blinded to all clinical information. Images were evaluated for the presence of osseous lesions, which were differentiated in radiologically active lesions (RAL) and radiologically not active lesions (RNAL). RAL were defined as areas of increased signal intensity (SI) on STIR images and decreased SI lower than muscle on T1-w images. RNAL were defined as areas of decreased SI lower than muscle on T1-w images, which showed no signal alteration on STIR images or as abnormal vertebral deformities in the spine. In each exam, a number of lesions and their exact anatomic location were noted. Lesions were further evaluated for the presence of associated periosteal reaction-like thickening of the periosteum and/or adjacent soft tissue oedema and for the existence of adjacent hyperostotic changes like cortical thickening or bone expansion. Readers noted the extent of body coverage in all MRI scans and rated the image quality of all sequences as diagnostic or not diagnostic.

Radiologic index

As parameters of interest (POI) for the description of NBO appearance in WB-MRI, we defined the number of RAL, the diameter of the patients' maximum RAL, the presence of extramedullary involvement and the presence of spinal involvement.

The disease extent was classified according to the number of lesions as unifocal (single lesion present), paucifocal (two to four lesions present) and as multifocal (more than four lesions present). The maximum diameter of bone marrow oedema of each patient's largest RAL was measured on coronal STIR images. Lesions smaller than 10 mm were classified as minor lesions, lesions between 10 mm and 100 mm were classified as moderate lesions, whilst lesions larger than 100 mm were classified as major lesions.

Lesions with a periosteal reaction were classified as an acute form of extramedullary involvement. Lesions with hyperostotic changes were classified as chronic extramedullary involvement. The presence of RAL in the vertebral column was classified as active spinal involvement. The presence of a vertebral bone deformity was classified as chronic spinal involvement. We scored the POI 'number of RAL' and 'size of patient's maximum RAL' with 1-3 index points each. The POI 'active/chronic extramedullary involvement ' and 'active/chronic spinal involvement' were scored with one index point each. All POI added up to a maximum of 10 points. POI, descriptions, criteria and assigned index points can be seen in Table 2. This radiologic index for WB-MRI in patients with NBO was termed RINBO.

Statistical analysis

Continuous data are presented as mean ± standard deviation and categorical as frequency plus percentage, if not otherwise specified. Non-paired t-test and Fisher's Exact test were used to assess for differences within continuous and categorical variables, if not otherwise specified.

For the agreement concerning the presence and number of lesions of clinical and MR-based detection, non-weighted and weighted kappa were applied, respectively. Comparing lesions without and with anatomical matching correlates between clinical and MR-based detection, a mixed effects model with a random intercept was applied accounting for potential clustering effect of multiple lesions within one patient.

The Spearman correlation coefficient was used to determine correlation of RINBO with continuous parameters. To determine whether RINBO is a predictor for the presence of CAL, logistic regression models with Firth correction for monotone likelihood was applied. Based on these models, c-statistics was derived, which is equivalent to the area under the

Table 2 Suggestion of a radiologic index for WB-MRI in patients with NBO (RINBO)

Parameter of interest	Description	Criterion	Value
№ of radiologic active lesions (RAL)	unifocal	1	1
	paucifocal	2-4	2
	multifocal	≥5	3
Maximum size of patient's RAL	minor	<10 mm	1
	average	≤100 mm	2
	major	>100 mm	3
Extramedullary affection	acute	periosteal reaction and/or adjacent soft tissue edema	1
	chronic	hyperostosis	1
Spine involvement	acute	radiologically active spine lesion	1
	chronic	NBO related vertebral body deformation	1
Maximum index points			10

receiver-operating characteristics curve (AUC) as a measure for discriminative power.

All performed tests were two-sided and performed with SAS (version 9.4, SAS Institute Inc., Cary, NC). A p-value <0.05 was considered statistically significant.

Results

Study cohort and clinical presentation

The study cohort consisted of 40 patients (68 % female, age 19 ± 9 years, range 8-60 years) diagnosed with NBO, Table 3. Thirty patients (75 %) yielded CAL, on average 2.1 ± 1.6 (range 1-8) lesions per patient (lpp). Lesions were anatomically distributed as shown in Table 4. Ten patients (25 %) did not present with CAL at the time of examination, but shared a history of NBO defining clinical symptoms in their past. No significant differences were observed between patients with and without CAL regarding age ($p = 0.46$) and gender ($p = 1.00$). Mean value of VAS of symptomatic patients was 4.0 ± 3.5.

Findings of WB-MRI

All patients underwent MR scanning without any adverse events (standard protocol scan time 41 ± 7 mins). Unlimited full body coverage was achieved in 43 % of the patients ($n = 17$), restricted coverage excluding part of the upper extremities in 58 % ($n = 23$; 15 elbow, 16 distal radius) and excluding the patient's feet in 5 % ($n = 2$). Reduced diagnostic image quality of the coronal STIR weighted images of the upper thoracic section was observed in 13 % ($n = 5$) due to breathing-artefacts; otherwise all images were of diagnostic image quality.

Table 3 Demographic data of study group

	Female	Male	All
Number of patients	27	13	40
Mean age [y] (±SD)	19 ± 7	19 ± 13	19 ± 9

33 patients demonstrated a total of 95 RAL (2.9 ± 1.9 lpp) plus additionally 13 RNAL. Two patients had only RNAL (one and three) and five patients did not have any radiologic lesion. The most common anatomic locations were long tubular bones (85 % metaphyseal, 46 % epiphyseal, 7 % diaphyseal), pelvis and spine; Table 4. Lesions appearance varied from botchy to ill-defined or confluent areas of bone marrow oedema; Fig. 1. Periosteal reaction was found in 23 % ($n = 22$) of RAL**;** Fig. 1. Hyperostotic changes were found in 12 of 112 lesions (11 %). The size of each patient's largest RAL was 63.8 ± 54.6 mm (largest lesion: 265 mm). Symmetric lesions were detected in 16 patients (40 %), who were on average younger than patients without symmetric lesions (15.1 ± 6.3 vs. 21.6 ± 10.0 years, $p = 0.03$, respectively). RAL in the spine were found in seven patients (18 %) with no significant association with age or gender (all $p \geq 0.65$); Fig. 2. Loss of vertebral body height was observed in eight patients (20 %) including six patients with vertebra plana formation.

Correlation of clinical and WB-MRI findings

On a per-patient level, the kappa for presence of active lesions was 0.33 ± 0.17. Whilst three patients had CAL without demonstrating RAL, six patients had RAL without showing CAL. Comparing the number of active lesions as detected clinically to radiologically, the weighted kappa was 0.22 ± 0.10. In 45 % of the cohort, more active lesions were detected by WB-MRI than by clinical examination whilst in 18 % less lesions were detected. No difference was observed between these two groups regarding age, gender or time interval between clinical and MRI examination (all $p \geq 0.12$). Taking also RNAL into

Table 4 Anatomic distribution of lesions and local radiological and clinical prevalence in the patient group ($n = 40$)

Lesion sites	№ of RAL of all patients	№ of RNAL of all patients	№ of CAL of all patients	№ and % of patients showing radiologic lesions		№ and % of patients showing CAL	
Whole body	95	17	62	35	88%	30	75%
Mandible	2	0	1	2	5%	1	3%
Zygomatic bone	0	0	1	0	0%	1	3%
Clavicle	6	0	5	6	15%	5	13%
Sternum	3	0	5	3	8%	5	13%
Proximal humerus	0	0	1	0	0%	1	3%
Distal radius	3	0	1	2	5%	1	3%
Pelvis	21	3	9	16	40%	5	13%
Proximal femur	4	2	8	5	13%	6	15%
Distal femur	9	0	2	6	15%	2	5%
Proximal tibia	12	0	9	8	20%	8	20%
Distal tibia	12	1	6	8	20%	6	15%
Distal fibula	1	0	0	1	3%	0	0%
Foot	8	1	4	3	8%	3	8%
Cervical vertebra	0	1	1	1	3%	1	3%
Thoracic vertebra	13	9	9	9	23%	5	13%
Lumbar vertebra	0	0	0	0	0%	0	0%

account, in 75 % more lesions were detected on MRI than by clinical examination.

For detecting RAL in the spine, kappa was 0.61 ± 0.18 on a per-patient level. Three patients had no acute clinical symptoms in the spine but RAL; Table 5. Vertebra plana formation was not associated with local clinical symptoms in four of six patients.

In 42 % ($n = 61$) of all detected, active lesions (clinically or radiologically, $n = 146$) demonstrated a direct correlate in the other detection modality. Shoulder girdle lesions were more likely to show a positive, anatomical match ($p = 0.009$); in contrast for foot lesions a tendency was observed to match less likely ($p = 0.07$); Table 6. Lesions tended to match less likely in young patients (age of 16.6 ± 6.3 years for patients with lesions without a matching correlate vs. age of 19.9 ± 8.5 years for patients with lesions with a matching correlate, $p = 0.05$), Table 6.

Radiologic Index

The on experts' opinion based derivation algorithm for the RINBO is detailed in Table 2. Patients' score in RINBO ranged from 0 to 8 (4.3 ± 2.3). The RINBO score correlated negatively with age ($r = -0.37$, $p = 0.02$) and did not differ significantly between genders (5.1 ± 1.9 vs. 3.9 ± 2.4 for male and female, $p = 0.14$). No correlation was observed between RINBO and VAS ($r = 0.02$, $p = 0.90$). RINBO was significantly higher in patients with CAL than without (4.8 ± 2.0 vs 2.8 ± 2.6, $p = 0.01$). Accordingly, RINBO was a significant predictor for the presence of CAL (OR 1.4 [95%CI: 1.03-1.98]) with an AUC of 0.705.

Serum biomarkers

Mean values of ESR were 21.7 ± 17 mm/1 h and 43.4 ± 25 mm/2 h and mean value of CRP was 0.7 ± 1.0 mg/dl. They were pathologic in 67 % and 31 %, respectively, of the patient subset with laboratory tests. ESR was significantly more frequently pathologic in patients with CAL than without (76 % vs. 0 %, $p = 0.03$ respectively). ESR was more strongly related to CAL than CRP. CRP demonstrated a significant difference between patients with and without RAL (0.8 ± 1.0 vs. 0.2 ± 0.1 mg/L, $p = 0.01$, respectively), whilst ESR measures did not (all $p \geq 0.08$).

Discussion

WB-MRI is increasingly being implemented in the diagnostic work-up of NBO, where it offers an attractive non-ionizing, ALARA-proof alternative to bone scintigraphy for its usually young patient collective [17–19, 23, 24].

We could demonstrate that WB-MRI with a scanning time of approximately 40 minutes is well-tolerated even by children and achieves an adequate image quality in the vast majority of examinations (88 %). An implementation of less breathing susceptible sequences and additional transverse STIR sequence covering this critical area could be discussed as a possible means of protocol optimization. Like predescribed (26), it was hard to adequately delineate elbows, hands or feet in some exams; therefore, we recommend applying special scrutiny here to achieve appropriate image quality.

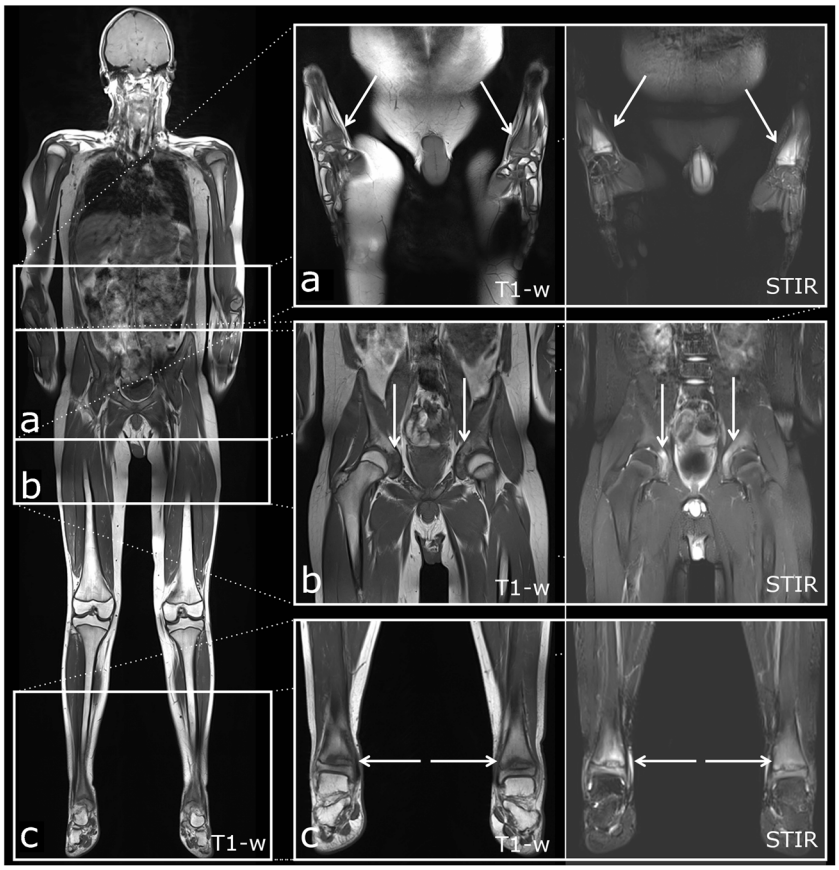

Fig. 1 Composed, coronal Whole-body MRI images in T1 weighting (left side) of a 14-year-old male patient presenting with clinically symptomatic lesions in the left distal radius and the right distal tibia **a** Enlarged coronal sections in T1 and STIR weighting of the distal upper extremities reveal profound bone marrow oedema in the distal metaphysis and epiphysis of the distal radius on both sides consistent with symmetric radiologically active lesions (oblique white arrows). Increased signal intensity in STIR weighting can be distinguished in the soft tissue laterally to the distal radius on the left representing reactive oedema and therefore soft tissue involvement. **b** Enlarged coronal sections in T1 and STIR weighting of the pelvis reveal extensive bone marrow oedema along the acetabulum bilaterally consistent with symmetric radiologically active lesions (vertical white arrows). **c** Enlarged coronal sections in T1 and STIR weighting of the distal lower extremities reveal bone marrow oedema in the distal metaphysis of the tibia accentuated to the right consistent with symmetric radiologically active lesions (horizontal white arrows)

Fig. 2 Whole-body MRI images of the spine of a 12-year-old male patient, asymptomatic at the time of examination. **a** and **c** Composed sagittal images of the spine in T1 weighting and in STIR weighting reveal height loss of the vertebral bodies T9 and T10 in the lower thoracic spine (broad white arrow). **b** and **d** Enlarged coronal and sagittal sections in T1 weighting and STIR weighting show pronounced height loss of T9 with subtle oedema (rectangular white arrow) and subtle height loss of T10 with pronounced oedema (oblique white arrow)

Table 5 Whole body MRI data variables of patient cohort and of patient groups with clinically active lesions and without clinically active lesions listed with their related *p*-values after testing for differences

	All patients	Patients with clinically active lesions	Patients without clinically active lesions	*p*-value
N	40	30	10	
Time interval between clinical exam und MRI [in days]	8 ± 22	8 ± 23	9 ± 17	0.87
Presence of radiologically active lesions	83 % (33)	90 % (27)	60 % (6)	0.052
Presence of radiological spine lesions (active only)	18 % (7)	13 % (4)	30 % (3)	0.34
Presence of radiological symmetric lesions (active only)	40 % (16)	47 % (14)	20 % (2)	0.26
Presence of radiologically non-active lesions	28 % (11)	23 % (7)	40 % (4)	0.01
Presence of radiological lesions (active or non-active)	88 % (35)	97 % (29)	60 % (6)	0.01
Number of radiologically active lesions	2.4 ± 2.0	2.7 ± 2.1	1.4 ± 1.4	0.08
Number of radiologically non-active lesions	2.8 ± 2.1	3.0 ± 2.1	2.1 ± 2.2	0.24
Number of radiological lesions (active or non-active)	5.2 ± 4.1	5.7 ± 4.2	3.5 ± 3.5	0.14

Lesions' predilection for the metaphyses of the long bones of the lower extremities, involvement of mandible, clavicle, sternum, pelvis and spine and variable appearance of bone marrow oedema met the described morphologic appearance of NBO [17–19, 25]. With 2.1 CAL per symptomatic patient, the number of clinically affected sites in our study was in agreement with previously published data [18]. With 95 RAL in 33 patients (2.9 lpp / mean age 17 years) we deviate from previous trials (7.8 lpp / mean age 13 years [18] or 9.6 lpp / mean age 11 years, respectively [19]), Differences could be explained by the inverse association between the number of RAL and the patients' age ($r = -0.38$, $p = 0.01$) and may indicate that younger patients in particular would benefit from WB-MRI. The prevalence of periosteal reactions / symmetric bone lesions was noticeable / significantly lower in our study than in others (23 % vs 32 % [19] or 48 % [18] and 40 % vs. 75 % [19] or 85 % [18]), which could lead to the hypothesis that periosteal reactions are less frequent in older patients and that some lesions fully disappear during the course of the disease.

The regular spine involvement of nearly a fifth of our cohort highlights the possible role that WB-MRI findings can have in the clinical management of NBO, as it leads several authors to recommend drug therapy with Pamidronate [26, 27] which is assumed to help in preserving mechanical stability, preventing vertebral collapse and consecutive acute neurologic or life time orthopaedic problems [28, 29].

Our study is the first to directly correlate clinical appearance of NBO patients with WB-MRI findings in a larger cohort ($n = 40$) (c.p. Fritz et. Al. [18]; $n = 13$). With a kappa of 0.33 for the presence of active lesions we found a fair agreement of WB-MRI and clinical examination.

The absence of radiologic correlates in three symptomatic patients could not be sufficiently explained by the time interval between the examinations (>5 days in only one patient) but could indicate pain amplification syndrome, which has an important impact on the clinical management as drug therapy is of limited value.

Our data confirms the potential of WB-MRI to detect subclinical lesions (six asymptomatic patients revealing RAL; nearly three fourths of patients with more lesions discovered by WB-MRI than clinically) including the spine (three of seven patients with RAL asymptomatic) [17].

Table 6 Radiologically active lesions without and with anatomical matching correlate; #accounted for clustered effect

	All radiologically active lesions	Anatomical Mismatch	Anatomical Match	*p*-value[#]
Age		16.6 ± 6.3	19.9 ± 8.5	0.052
Male	28 %	32 %	23 %	0.63
Anatomic Locations				
Long bones	47 %	45 %	51 %	0.65
Pelvis	18 %	22 %	13 %	0.20
Spine	13 %	13 %	13 %	0.72
Shoulder girdle	10 %	4 %	18 %	0.009
Foot	9 %	14 %	2 %	0.07
Others (knee, face)	3 %	2 %	3 %	0.87

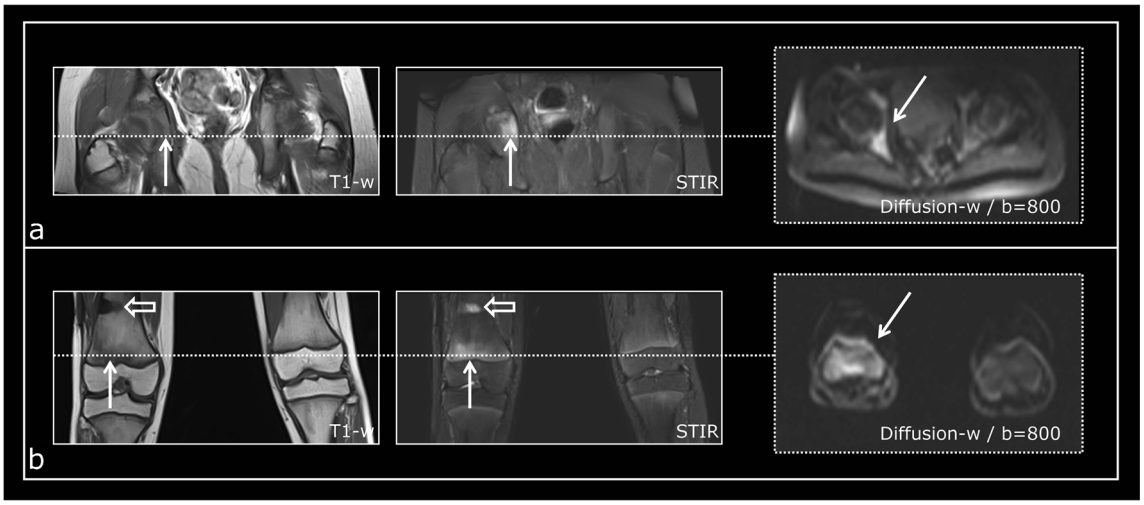

Fig. 3 Whole-body MRI images of a 13-year-old male patient presenting with clinically active lesions in the right pelvis and the right knee. **a** Focused coronal sections in T1 and STIR weighting reveal bone marrow oedema in the right acetabulum (white vertical arrow). Perpendicular axial section in Diffusion weighted imaging technique shows distinct corresponding signal increase in b = 800 images (oblique white arrow). **b** Focused coronal sections in T1 and STIR weighting reveal bone marrow oedema in the distal metaphysis of the right femur (white vertical arrow). Altered signal adjacent to a cortical defect more proximally in the right femur is in keeping with the status after bone biopsy (hollow white arrow). Perpendicular axial section in diffusion weighted imaging technique shows distinct corresponding signal increase in b = 800 images (oblique white arrow)

The noticeable anatomical match between CAL and RAL in the shoulder girdle could lead to the assumption that lesions here are either being well detected despite local limitations in image quality or are more likely to be symptomatic. Poor anatomical match in the feet can justify targeted MRI, if findings are inconclusive in this hard to interpret location [30].

Besides the STIR imaging technique, that we used in our study, diffusion weighted imaging (DWI) offers an alternative method for the detection of bone marrow oedema [31]. In DWI sequences with b values of 800, which covered some of our patients' RAL, we could prove high signal intensity within the NBO lesions; Fig. 3. In the light of these promising findings, we recommend that future studies test the value of whole body DWI including ADC mapping in the setting of NBO.As laboratory markers again [18, 32] presented as inconclusive, WB-MRI in our opinion is a very attractive method for diagnosing, staging and follow-up of NBO. To facilitate its implementation, we devised the new radiologic index RINBO. The purpose of RINBO is to encourage standardized reporting, improve reproducibility and ease stratification of WB-MRI findings, therefore, following recent trends in radiology research [33].

Applied in our patient group, RINBO was a significant predictor for the presence of CAL, which supports the idea of RINBO to offer a representative means to grade the affective intensity of disease and to simplify the evaluation of progression, stability or remission during the course of disease. Beyond that, RINBO might provide terms of reference for individualized drug therapies and help to monitor treatment response. However, further validation is required, as we did not take into account patients' medication nor assessed follow-up scans. This and imaging analysis in consensus reading where inter- and intra-observer variation remains unknown are limitations of our study.

In conclusion, WB-MRI is a powerful method for the evaluation of disease burden and activity in patients with NBO, which may enable a more precise and accurate assessment of NBO and - using a standardized evaluation approach, such as the index RINBO - might allow for improving therapeutic decisions in NBO patients in the future.

Acknowledgments The scientific guarantor of this publication is PD Dr. Annette Jansson. The authors of this manuscript declare no relationships with any companies, whose products or services may be related to the subject matter of the article. The authors state that this work has not received any funding. One of the authors has significant statistical expertise. Institutional Review Board approval was obtained. Written informed consent was obtained from all subjects (patients) in this study. Some study subjects or cohorts have been previously reported in: Voit AM, Arnoldi AP, Douis H et al (2015) Whole-body Magnetic Resonance Imaging in Chronic Recurrent Multifocal Osteomyelitis: Clinical Longterm Assessment May Underestimate Activity. J Rheumatol 42:1455-1462. Methodology: prospective, diagnostic study, performed at one institution.

References

1. Jansson A, Renner ED, Ramser J et al (2007) Classification of non-bacterial osteitis: retrospective study of clinical, immunological and genetic aspects in 89 patients. Rheumatology (Oxford) 46:154–160
2. Jansson AF, Grote V, Group ES (2011) Nonbacterial osteitis in children: data of a German Incidence Surveillance Study. Acta Paediatr 100:1150–1157

3. Giedion A, Holthusen W, Masel LF, Vischer D (1972) Subacute and chronic "symmetrical" osteomyelitis. Ann Radiol (Paris) 15: 329–342
4. Hofmann SR, Roesen-Wolff A, Hahn G, Hedrich CM (2012) Update: Cytokine Dysregulation in Chronic Nonbacterial Osteomyelitis (CNO). Int J Rheumatol 2012:310206
5. Golla A, Jansson A, Ramser J et al (2002) Chronic recurrent multifocal osteomyelitis (CRMO): evidence for a susceptibility gene located on chromosome 18q21.3-18q22. Eur J Hum Genet 10: 217–221
6. Bjorksten B, Boquist L (1980) Histopathological aspects of chronic recurrent multifocal osteomyelitis. J Bone Joint Surg (Br) 62:376–380
7. Deltombe T, Nisolle JF, Boutsen Y, Gustin T, Gilliard C, Hanson P (1999) Cervical spinal cord injury in sapho syndrome. Spinal Cord 37:301–304
8. Girschick HJ, Huppertz HI, Harmsen D, Krauspe R, Muller-Hermelink HK, Papadopoulos T (1999) Chronic recurrent multifocal osteomyelitis in children: diagnostic value of histopathology and microbial testing. Hum Pathol 30:59–65
9. Girschick HJ, Raab P, Surbaum S et al (2005) Chronic non-bacterial osteomyelitis in children. Ann Rheum Dis 64:279–285
10. Jurik AG, Egund N (1997) MRI in chronic recurrent multifocal osteomyelitis. Skelet Radiol 26:230–238
11. Bamberg F, Parhofer KG, Lochner E et al (2013) Diabetes mellitus: long-term prognostic value of whole-body MR imaging for the occurrence of cardiac and cerebrovascular events. Radiology 269: 730–737
12. Schmidt GP, Reiser MF, Baur-Melnyk A (2009) Whole-body MRI for the staging and follow-up of patients with metastasis. Eur J Radiol 70:393–400
13. Schmidt GP, Reiser MF, Baur-Melnyk A (2009) Whole-body imaging of bone marrow. Semin Musculoskelet Radiol 13:120–133
14. Weckbach S (2009) Whole-body MR imaging for patients with rheumatism. Eur J Radiol 70:431–441
15. Weckbach S (2012) Whole-body MRI for inflammatory arthritis and other multifocal rheumatoid diseases. Semin Musculoskelet Radiol 16:377–388
16. Weckbach S, Schewe S, Michaely HJ, Steffinger D, Reiser MF, Glaser C (2011) Whole-body MR imaging in psoriatic arthritis: additional value for therapeutic decision making. Eur J Radiol 77: 149–155
17. Falip C, Alison M, Boutry N et al (2013) Chronic recurrent multifocal osteomyelitis (CRMO): a longitudinal case series review. Pediatr Radiol 43:355–375
18. Fritz J, Tzaribatchev N, Claussen CD, Carrino JA, Horger MS (2009) Chronic recurrent multifocal osteomyelitis: comparison of whole-body MR imaging with radiography and correlation with clinical and laboratory data. Radiology 252:842–851
19. von Kalle T, Heim N, Hospach T, Langendorfer M, Winkler P, Stuber T (2013) Typical patterns of bone involvement in whole-body MRI of patients with chronic recurrent multifocal osteomyelitis (CRMO). Röfo 185:655–661
20. Fritz J (2015) The contributions of whole-body magnetic resonance imaging for the diagnosis and management of chronic recurrent multifocal osteomyelitis. J Rheumatol 42:1359–1360
21. Jansson AF, Muller TH, Gliera L et al (2009) Clinical score for nonbacterial osteitis in children and adults. Arthritis Rheum 60: 1152–1159
22. Voit AM, Arnoldi AP, Douis H et al (2015) Whole-body magnetic resonance imaging in chronic recurrent multifocal osteomyelitis: clinical longterm assessment may underestimate activity. J Rheumatol 42:1455–1462
23. Voss SD, Reaman GH, Kaste SC, Slovis TL (2009) The ALARA concept in pediatric oncology. Pediatr Radiol 39:1142–1146
24. Strauss KJ, Kaste SC (2006) The ALARA (as low as reasonably achievable) concept in pediatric interventional and fluoroscopic imaging: striving to keep radiation doses as low as possible during fluoroscopy of pediatric patients–a white paper executive summary. Pediatr Radiol 36:110–112
25. Jurik AG (2004) Chronic recurrent multifocal osteomyelitis. Semin Musculoskelet Radiol 8:243–253
26. Roderick M, Shah R, Finn A, Ramanan AV (2014) Efficacy of pamidronate therapy in children with chronic non-bacterial osteitis: disease activity assessment by whole body magnetic resonance imaging. Rheumatology (Oxford) 53:1973–1976
27. Hospach T, Langendoerfer M, von Kalle T, Maier J, Dannecker GE (2010) Spinal involvement in chronic recurrent multifocal osteomyelitis (CRMO) in childhood and effect of pamidronate. Eur J Pediatr 169:1105–1111
28. Armstrong A, Upadhyay N, Saxby E, Pryce D, Steele N (2013) Chronic recurrent multifocal osteomyelitis causing an acute scoliosis. Case Rep Pediatr 2013:649097
29. Baulot E, Bouillien D, Giroux EA, Grammont PM (1998) Chronic recurrent multifocal osteomyelitis causing spinal cord compression. Eur Spine J 7:340–343
30. Weishaupt D, Schweitzer ME (2002) MR imaging of the foot and ankle: patterns of bone marrow signal abnormalities. Eur Radiol 12: 416–426
31. Neubauer H, Evangelista L, Morbach H et al (2012) Diffusion-weighted MRI of bone marrow oedema, soft tissue oedema and synovitis in paediatric patients: feasibility and initial experience. Pediatr Rheumatol Online J 10:20
32. Wipff J, Adamsbaum C, Kahan A, Job-Deslandre C (2011) Chronic recurrent multifocal osteomyelitis. Joint Bone Spine 78:555–560
33. Schwartz LH, Panicek DM, Berk AR, Li Y, Hricak H (2011) Improving communication of diagnostic radiology findings through structured reporting. Radiology 260:174–181